Journal of Materials Chemistry C

ROYAL SOCIETY OF CHEMISTRY

PAPER

View Article Online
View Journal | View Issue

Cite this: J. Mater. Chem. C, 2022, 10, 13834

Lithium-ion distribution and motion in two-dimensional covalent organic frameworks: the example of TAPB-PDA COF†

Hanyin Zhang[ab] and Haoyuan Li *[ac]

Two-dimensional covalent organic frameworks (2D COFs) are promising as solid-state electrolytes due to their high structural stability, lack of glass transition temperature, and molecular versatility. For more rational molecular and system design toward better ionic conduction in COFs, a detailed understanding of the ion distributions, ionic motions, and interactions among different species is needed. Achieving this goal requires insights at the molecular level, where computer simulations can be a powerful tool. However, efficient protocols that can model lithium-ion trajectories in COFs over long times are still to be explored, which are needed for the reliable consideration of Li^+ motions as well as for the development of high-throughput molecular screening strategies for accelerated materials discovery. Here, we apply molecular dynamics simulations with electronic continuum correction to study lithium-ion distributions and motions in 2D COFs. The efficient force fields have allowed us to model trajectories over hundreds of nanoseconds and the consideration of experimentally relevant lithium loading. The imine-linked TAPB-PDA COF, which has become a model system in COF-related studies, is taken here as an example. $LiClO_4$ is used to provide Li^+, and the role of propylene carbonate is studied. Our analysis provides a comprehensive understanding of the distributions and motions of lithium ions and anions. It was found that $LiClO_4$ tends to form clusters that attach to the walls of COF pores that limit ionic motions. The addition of propylene carbonate molecules helps the dispersion of Li^+ in the COF pores for increased mobility. These results highlight the role of microscopic interactions between different components and point to potential optimization directions for higher ionic conductivity engineering of 2D COFs.

Received 17th March 2022,
Accepted 16th May 2022

DOI: 10.1039/d2tc01076c

rsc.li/materials-c

1. Introduction

The fast development of electric vehicles and grid-scale energy storage systems demands post lithium-ion batteries (LIBs) with high energy and power density. All-solid-state Li batteries are particularly attractive as they have superior energy density compared to commercial lithium-ion batteries due to the high theoretical specific capacity of lithium metal of 3860 mA h g^{-1} (in comparison to 374 mA h g^{-1} for the commercial graphite anode).[1–5] To obtain Li metal batteries with high performances, it is essential to develop solid electrolytes (SEs) with high Li^+ conductivities and stability.[6,7] One of the most promising SEs discovered in recent years is two-dimensional covalent organic frameworks (2D COFs).[8–16] They are a type of highly versatile, porous material with atomically precise, nanometer-sized pores and can be integrated with designed functional groups for electron conduction and ion transport.[17–21] As SEs, stacked 2D COFs form open channels for ion transport, and the lack of a glass transition temperature makes them ideal for working in a wide temperature range.[22] However, the Li^+ conductivities of pristine COFs often do not exceed the order of 10^{-5} S cm^{-1} at room temperature, compared to 10^{-3} S cm^{-1} of liquid organic electrolytes.[12,23–25] These low ion conductivities have largely limited their applications as SEs. Ultimately improving COFs for their successful application in Li metal batteries requires a thorough understanding of the ion transport mechanism as well as the molecular structures and interactions in these COF-based systems, which, unfortunately, remains largely unclear. For example, it is known that lithium ions do not occupy the entire available space in the COF framework. Instead, these COFs often have a lithium loading from 0.2 to 4% with ions

[a] Key Laboratory of Advanced Display and System Applications, Ministry of Education, Shanghai University, Shanghai 200072, China. E-mail: lihaoyuan@shu.edu.cn
[b] School of Materials Science and Engineering, Guangdong Provincial Key Laboratory of Advanced Energy Storage Materials, South China University of Technology, Guangzhou 510640, China
[c] School of Microelectronics, Shanghai University, Shanghai 201800, China

† Electronic supplementary information (ESI) available. See DOI: https://doi.org/10.1039/d2tc01076c

provided by salts such as $LiClO_4$.[8,11,16] Still, questions such as how the Li ions are distributed inside the COFs and how they move in the pores remain largely unanswered. Recently, propylene carbonate (PC), which originally functions as a liquid organic electrolyte, has been mixed into the Li^+–COF composite and found beneficial to ionic conduction.[11,26] Although this steps away from the all-solid-state design direction, understanding the role of PC can potentially offer insights for the development of strategies for good all-solid-state COF ionic conductors. At present, knowledge of how those lithium ions of a few percentages are distributed and move across the COF pores and how COFs/other components interact with Li^+ can be of great value to developing molecular and system design strategies for COF-based ionic conductors.

While it remains challenging to accurately probe the distribution and motion of lithium ions inside 2D COFs using experimental techniques, computer simulations have proven useful. For example, density functional theory calculations can be used to study the optimal Li^+ configuration and energy barriers along the migration pathway.[10] *Ab initio* molecular dynamics simulations have also been explored to model Li^+ in COF-5 over trajectories of a few ps.[27] However, *ab initio*-based methods are often limited to small sizes and short time scales (ps) due to the demanding computational cost, while lithium-ion motion across multiple sites in COFs is estimated to be on nanosecond time scales. The high computational cost also poses a challenge in modeling ion transport in COF systems in an efficient manner, thus being ineffective in aiding material design. At this stage, it is of great value to explore efficient protocols that can model Li^+ in COFs for long times, which are crucial to the reliable consideration of Li^+ distributions and motions and beneficial to developing high-throughput molecular screening methods for accelerated materials discovery.

Molecular dynamics (MD) simulations based on the efficient classical force field are promising to model longer times and larger sizes, which have been successfully applied to the study of the structural features of 2D COF systems of tens of nm and at tens of ns.[28,29] Here, we apply molecular dynamics simulations to investigate lithium-ion transport in imine-linked COFs using TAPB-PDA COF as an example, which has become a model system in COF-related studies[30–32] and the force field parameters of which have been well established.[33,34] The electronic continuum correction (ECC) allows taking into account implicitly the polarization effect within the efficient force fields.[35,36] Different amounts of propylene carbonate were considered to understand its impact on Li^+ distribution and motion. The efficient simulations have allowed us to model systems with experimentally relevant Li loading and PC ratios for trajectories up to 200 ns. The simulations revealed the molecular interactions among Li^+, anions, COFs, and PC molecules. It was found that $LiClO_4$ tends to form clusters inside the COF pores, which leads to noncontinuous Li^+ transport pathways and localized ionic motion. The addition of PC molecules leads to more uniform distributions of lithium ions and makes it easier for them to move across the pores. The result is more continuous transport pathways and improved ionic conductivities.

Haoyuan Li

Dr Haoyuan Li is currently a Professor in the School of Microelectronics at Shanghai University in China. He obtained his PhD degree from Tsinghua University in 2015, under the supervision of Prof. Yong Qiu. He then joined the group of Prof. Jean-Luc Brédas as a Postdoctoral Fellow and became a Research Scientist later on. He worked at King Abdullah University of Science and Technology, Georgia Institute of Technology and the University of Arizona from 2015 to 2020. His research interests include two-dimensional covalent organic frameworks, organic electronic devices and energy storage systems by multi-scale simulations and machine learning modeling.

2. Methodologies

TAPB-PDA COF has eclipsed stacking with a layer distance of 3.5 Å.[31] Here, we consider multi-layer TAPB-PDA COF sheets in a co-facial configuration, and a $2 \times 2 \times 20$ supercell is constructed. Fig. 1 shows the top and side views of the supercell, which has 240 terephthalaldehyde (PDA) units and 160 1,3,5-tris(4-aminophenyl)benzene (TAPB) units. This structure is mixed with 240 $LiClO_4$ (one per PDA unit), corresponding to a lithium loading of 1.6 wt% and similar to the values used experimentally.[8,11,16] Different PC amounts that correspond to 10 wt%, 20 wt%, and 40 wt% in the final system were then added. The initial mixture structure was constructed using the PACKMOL package,[37] where $LiClO_4$ (and PC molecules) were randomly distributed in the available space in the COF framework. The chemical structures of TAPB-PDA COF and PC can be found in Fig. S1 in the ESI.†

Here, we utilize the all-atom optimized potentials for liquid simulations (OPLS-AA).[38] This force field has been shown to reproduce well the results of 2D COFs, including the TAPB-PDA COF at the density functional theory level in our previous works, in cases without external forces and at moderate applied stress.[33,34,39] The OPLS parameters of ClO_4^- were taken from the work of Acevedo and co-workers.[40] The atomic partial charges of ClO_4^- and PC were calculated using the ChelpG scheme[41] at the ωB97Xd/6-31G(d,p) level[42] for consistency with the parameters of TAPB-PDA COF.[33]

Electronic continuum correction allows for the reasonable description of charged particles by implicitly taking the electronic polarization effect while using the efficient classical force fields.[35,36] ECC has been successfully applied in studying chemistry- and biology-related problems, and recently, electrolytes for lithium-sulfur batteries.[36] The core idea of ECC is that

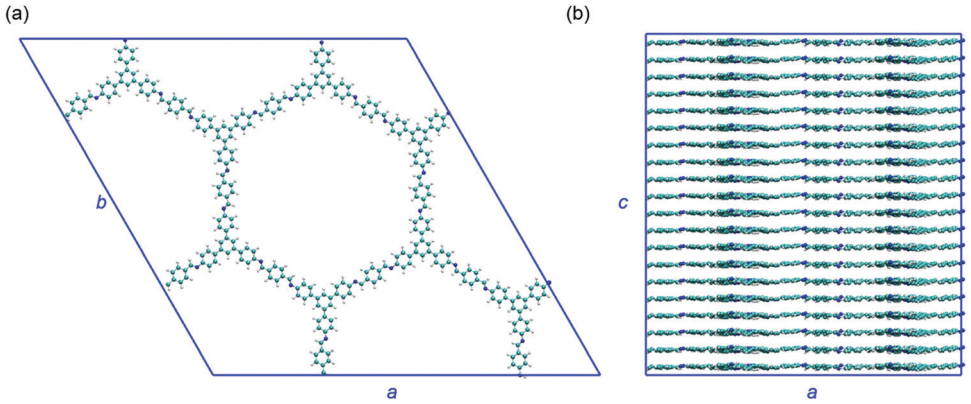

Fig. 1 (a) Top and (b) side view of the modeled 2 × 2 × 20 TAPB-PDA COF supercell. $a = b = 7.4$ nm, $c = 7.0$ nm, $\alpha = \beta = 90°$, $\gamma = 120°$. a and c are aligned with the x and z directions, respectively.

the corrected partial charge writes as:[43]

$$q_i^{ECC} = \frac{q_i}{\sqrt{\varepsilon_{el}}} \quad (1)$$

where ε_{el} is the high-frequency dielectric constant of the medium. In most relevant cases, ε_{el} is close to 2.[43] In our simulations, the partial charges for lithium ions and all atoms in ClO_4^- were scaled by 0.7. Our benchmarks show that the OPLS force field with this correction leads to a diffusion coefficient of lithium ions in propylene carbonate of 1.6×10^{-6} cm^2 s^{-1} (see Fig. S2 in the ESI†), which is within the experimental range of 1.2×10^{-6}–2.6×10^{-6} cm^2 s^{-1}.[44]

All MD simulations were performed using the GROMACS (2021.5) package.[45] The smooth particle–mesh Ewald (PME) method was used for electrostatic interactions.[46] The time step is 1 fs. The systems were brought to 298 K over 5 ns and simulated for 200 ns in total. The last 100 ns-trajectory was used for analysis. Velocity rescaling[47] and Nose–Hoover[48] thermostats were used for equilibrium and production simulations, respectively. For each system, snapshots of the structures were saved every 0.1 ns. The coordinates of COFs, Li^+, ClO_4^-, and PC molecules were then extracted and used for further analysis.

The mean square displacement (MSD) of lithium ions is expressed as:[49]

$$MSD(t) = \frac{1}{N}\sum_{i=1}^{N} |\mathbf{r}_i(t) - \mathbf{r}_i(0)|^2 \quad (2)$$

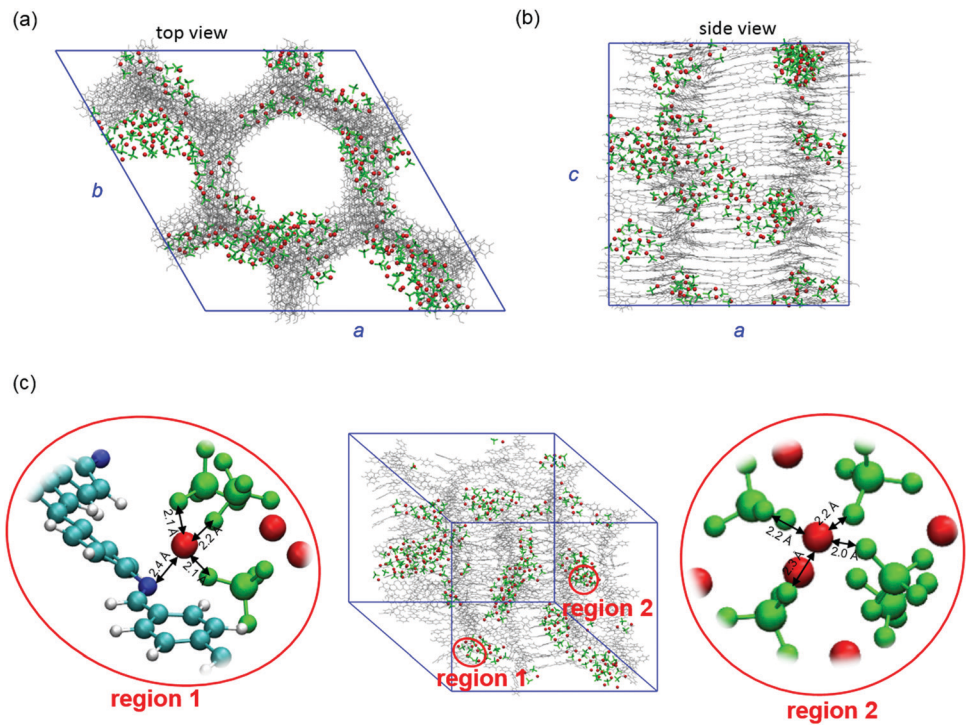

Fig. 2 (a) Top and (b) side view of the snapshot at 200 ns for TAPB-PDA COF mixed with $LiClO_4$. (c) A tilted view of the same structure with representative local structures of Li^+, ClO_4^-, and COF. Red spheres represent Li^+. Green spheres and rods represent ClO_4^-.

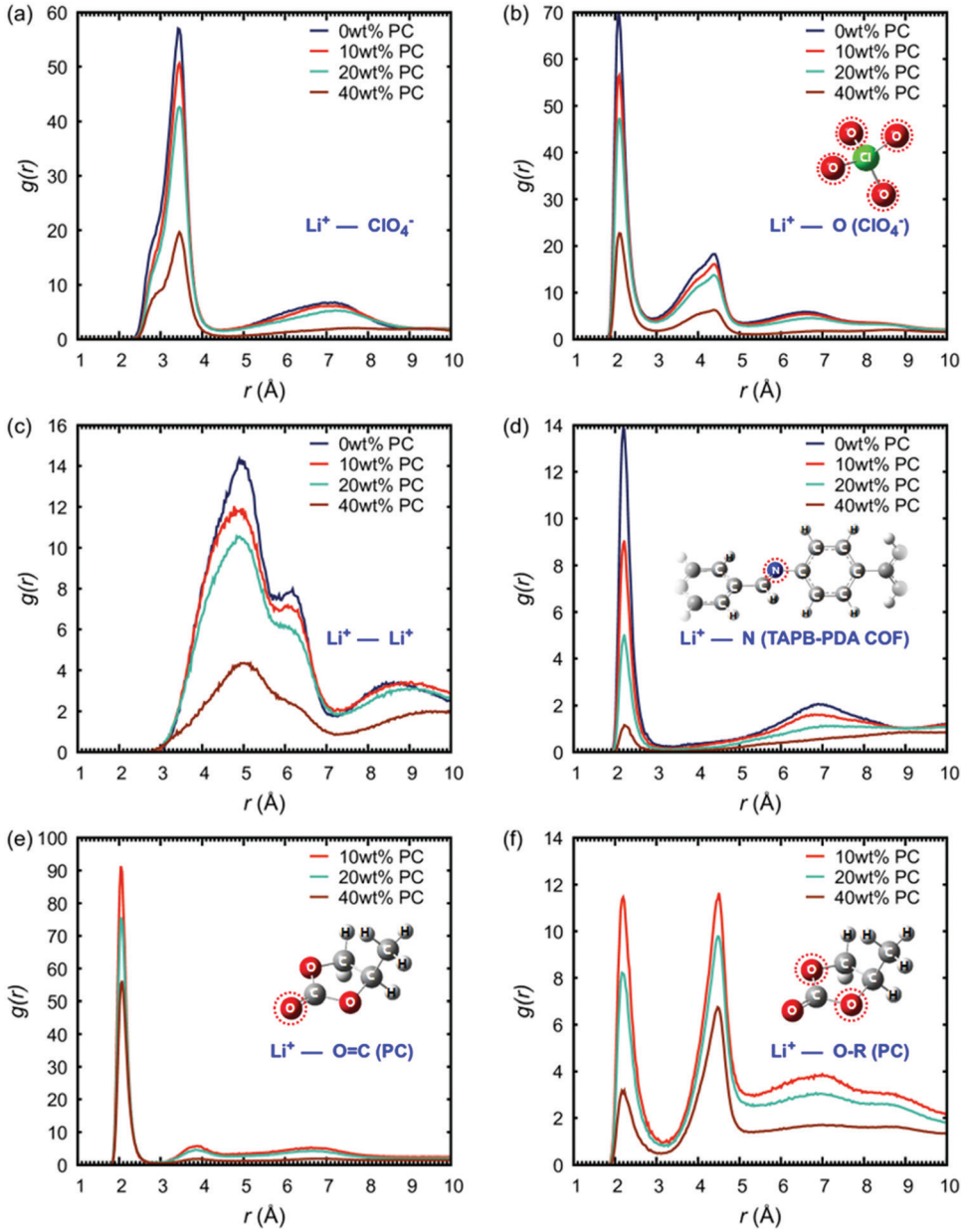

Fig. 3 Radial distribution functions of Li^+ and (a) the center of ClO_4^-, (b) the oxygen atoms in ClO_4^-, (c) Li^+, (d) N in the imine linkage, (e) O=C in PC, and (f) O–R in PC, respectively.

where N is the total number of lithium ions, and $\mathbf{r}_i(t)$ is the coordinate of lithium ion i at time t. Since we are mainly considering lithium-ion transport through the pores (in the z-direction), it is useful to use the one-dimensional version of eqn (2):

$$\mathrm{MSD}_{1D}(t) = \frac{1}{N}\sum_{i=1}^{N}\left|\mathbf{r}_{z,i}(t) - \mathbf{r}_{z,i}(0)\right|^2 \quad (3)$$

where $r_{z,i}$ is the coordinate of lithium ion i in the z-direction. The self-diffusion coefficient is then calculated as:[49]

$$D_{1D} = \frac{1}{2}\lim_{t\to\infty}\frac{\mathrm{MSD}_{1D}(t)}{t} \quad (4)$$

where t is time. The conductivity of lithium ions can be obtained based on the following relationship:[50]

$$\sigma_{Li^+} = \frac{e^2 c_{Li^+} D_{1D}}{k_B T} = \frac{1}{2}\frac{e^2 c_{Li^+}}{k_B T}\lim_{t\to\infty}\frac{\mathrm{MSD}_{1D}(t)}{t} \quad (5)$$

where e is the elementary charge, k_B is the Boltzmann constant, T is temperature, and c_{Li^+} is the concentration of Li^+.

3. Results and discussion

The simulations show that $LiClO_4$ forms clusters of a few nanometers, as illustrated in Fig. 2. The strong electrostatic interactions between ions Li^+ and ClO_4^- bind them closely

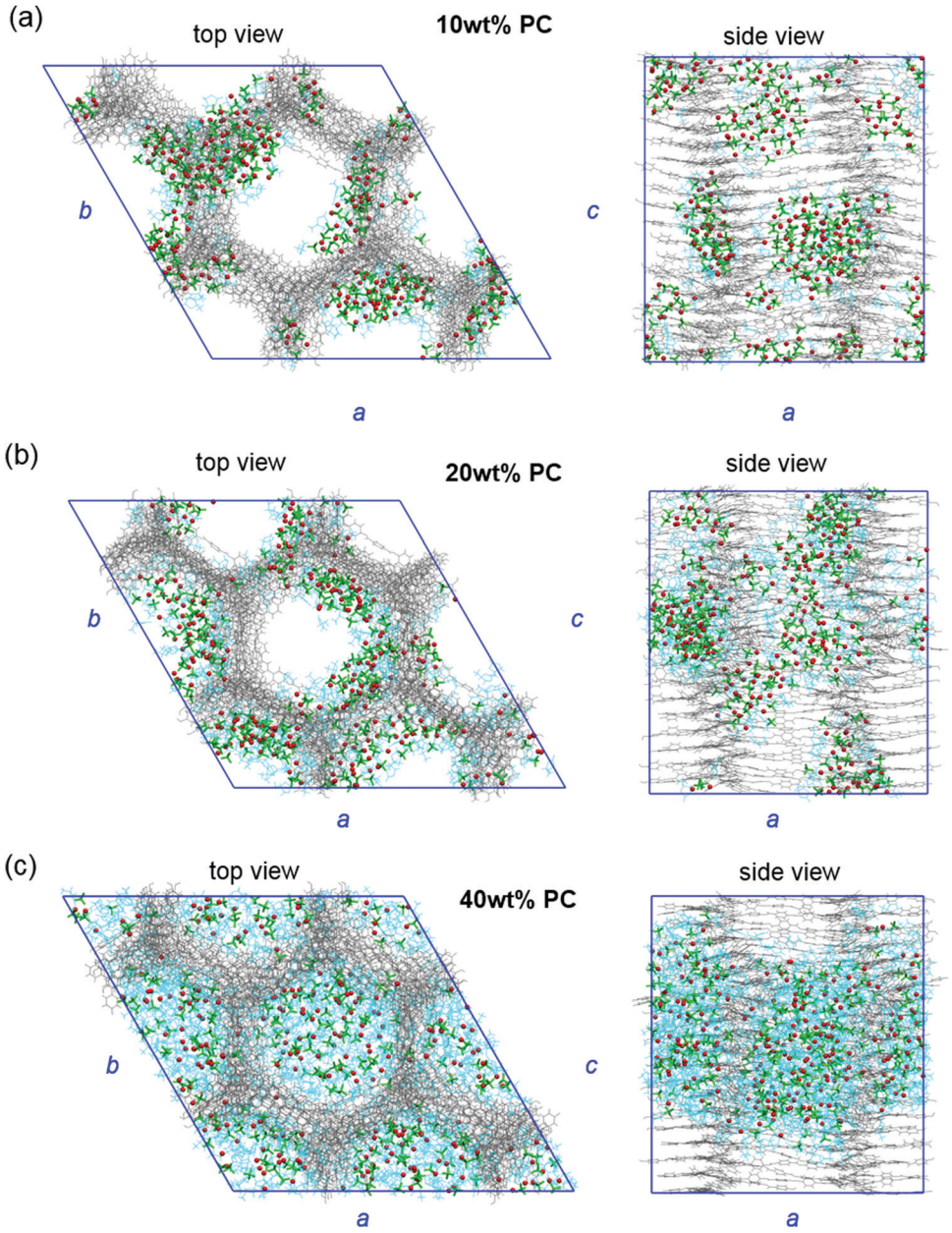

Fig. 4 Snapshots at 200 ns for TAPB-PDA COF mixed with $LiClO_4$ with (a) 10 wt%, (b) 20 wt% and (c) 40 wt% PC. Red spheres, green rods and cyan lines represent Li^+, ClO_4^- and PC molecules, respectively.

together. These clusters interact with the COF *via* van der Waals forces and are attached to the walls of the COF pores. We note that the $LiClO_4$ clusters do not penetrate the COF layers. As suggested in the radial distribution function $g(r)$ in Fig. 3(a), ClO_4^- forms shells around Li^+ with a typical center-of-mass distance of 3.4 Å. As for the corresponding atoms, Li^+ forms short contacts with the oxygen atoms in ClO_4^- with a strong peak at 2.1 Å (Fig. 3(b)), which agrees well with the value of ~2.0 Å from *ab initio* molecular dynamics simulations.[27] From Fig. 3(a) and (c), it can also be seen that the closest Li^+–Li^+ distance ranges from 3 Å to 7 Å, and a second ClO_4^- shell from the center Li^+ forms at ~6–8 Å. Overall, these data suggest that lithium ions are closely bound to the ClO_4^- counterion inside the $LiClO_4$ clusters. The strong peaks of the radial distribution functions in Fig. 3(a)–(c) at short distances and declining trends at long distances are consistent with the nanometer size of the $LiClO_4$ clusters. The radial distribution function in Fig. 3(d) suggests a contact around 2.2 Å between Li^+ and the nitrogen atoms in the imine linkage of the TAPB-PDA COF. Interestingly, the interaction between $LiClO_4$ and TAPB-PDA COF induces structural deformation of the COF and leads to increased degrees of layer mismatch (also see Fig. S3 and S4 in the ESI†). As Fig. 2(b) shows, the pore walls sink in the opposite direction of the attached $LiClO_4$ cluster.

Adding PC leads to more significant monomer unit displacement (Fig. S4, ESI†) and more loosely bound cations and

anions inside the TAPB-PDA COF. With increasing PC ratio, the peaks in the radial distribution functions in Fig. 3(a)–(c) get weaker at short ranges, which suggests increased distances among Li^+ and between Li^+ and ClO_4^-. As Fig. 4 demonstrates, Li^+ and ClO_4^- are well dispersed in the space where the PC molecules occupy, unlike in Fig. 2 where $LiClO_4$ forms localized clusters. At higher PC ratios, the Li^+–N peak in Fig. 3(d) also decreases, which suggests that more Li^+ are located away from the walls of the COF pores. On the other hand, the locations of the strongest peaks in Fig. 3(a)–(d) remain similar to those in the case without PC. This suggests that the local configurations of Li^+ that is still in contact with ClO_4^- and TAPB-PDA COF could remain similar. Li^+ interacts mainly with the oxygen atoms in PC, particularly the one that forms a double bond to C. This is demonstrated by the strong peak at 2.1 Å in the radial distribution function of Li^+ and O═C in Fig. 3(e). Furthermore, our data suggest that Li^+ tends to coordinate to PC in a side configuration instead of a top configuration, as shown in Fig. 5(a). The reason is as follows: a dominating top configuration would result in one prominent peak in the radial distribution function of Li^+ and O–R (PC), whereas most Li^+ coordinating in a side configuration leads to two prominent peaks as shown in Fig. 3(f). Representative structures of ClO_4^-- and PC-coordinated lithium ions are shown in Fig. 5(b) and (c).

The formation of $LiClO_4$ clusters in the absence of PC leads to localized distributions of the anions and cations in the TAPB-PDA COF. Indeed, as Fig. 6(a) illustrates, Li^+ and ClO_4^- only occupy a portion of the available space in TAPB-PDA COF in a non-continuous manner. Since Li^+ and ClO_4^- are closely bound, their occupations are largely overlapped. On the other hand, the distribution of PC molecules is more uniform, which suggests that they are more mobile than Li^+ and ClO_4^- and spread more easily into the TAPB-PDA COF pores. In addition, Li^+ and ClO_4^- are primarily distributed inside the PC region and form a good mixture, as shown in Fig. 6(b) and (c). As a result, the Li^+ and ClO_4^- distributions become more uniform and continuous pathways form, suggesting easier motion inside the COF pores.

The fact that $LiClO_4$ does not distribute uniformly in the COF pores and the absence of continuous lithium transport pathways can be detrimental to lithium-ion transport. The above discussions show that lithium ions are limited to their clusters or the PC region when present. As a result, when lithium ions approach the boundaries of $LiClO_4$ clusters (or the PC region), their motion may be slowed. To confirm this speculation, we quantify the ionic motion by calculating the MSD in the z-direction according to eqn (3) (we note that ion transport across the channel walls to an adjacent pore is unlikely since ions are not observed in between the COF sheets). As shown in Fig. 7(a), the increase of MSD of Li^+ with time slows down at longer distances, which agrees with the above speculation. A few other observations include: the mean square deviations of Li^+ and ClO_4^- are of similar strength, suggesting similar moving speeds; PC molecules are more mobile than Li^+ and ClO_4^-; increasing the amount of PC leads to larger MSDs for both Li^+ and ClO_4^-, which demonstrates increased ionic motions.

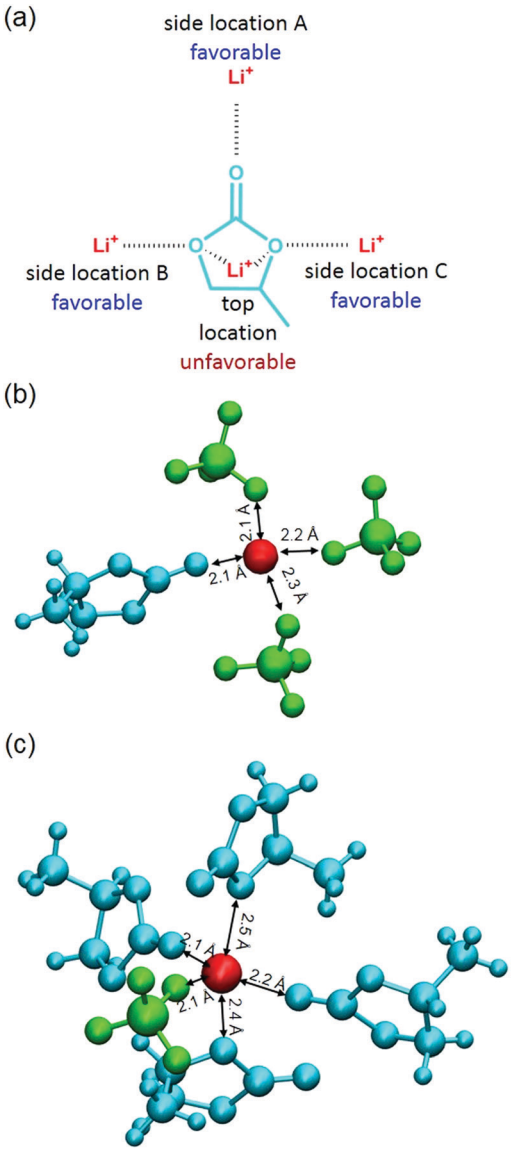

Fig. 5 Illustrations of (a) the Li^+-coordination site of PC and representative configurations of Li^+ (red) coordinated to ClO_4^- (green) and PC (cyan) in (b) the 20 wt% and (c) the 40 wt% PC systems.

The MSDs, while deviating from linearity over long time scales, can be used to shed light on the Li^+ conductivities. For the system without PC, σ_{Li^+} is roughly estimated to be 1.4×10^{-5} S cm^{-1} ($D_{1D} = 3.0 \times 10^{-9}$ cm^2 s^{-1}), while for the 40 wt% PC system it increases to 7.4×10^{-5} S cm^{-1} ($D_{1D} = 1.6 \times 10^{-8}$ cm^2 s^{-1}). These values are on similar orders to the reported experimental ionic conductivities of COFs.[12,25] The addition of PC molecules leads to increased ionic conductivity, highlighting its beneficial effect on promoting the motion of lithium ions in TAPB-PDA COF.

Since the motion of Li^+ is largely limited to the $LiClO_4$ clusters or the PC regions, it is likely that the movement of lithium ions over long distances inside the COF pores could proceed with the help of migration of the $LiClO_4$ clusters or the PC regions. To further improve the ionic conductivity of COFs,

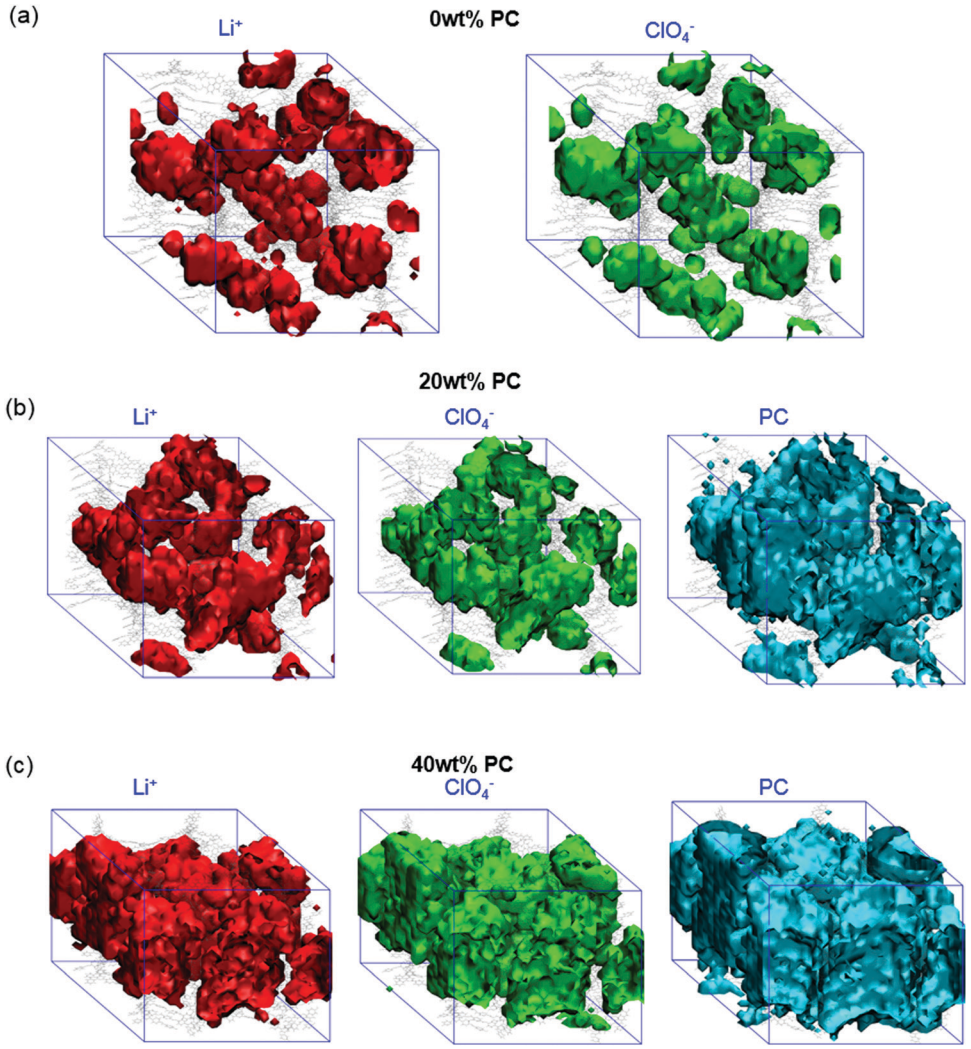

Fig. 6 Illustrations of the occupations of Li^+, ClO_4^- and PC at (a) 0 wt%, (b) 20 wt% and (c) 40 wt% PC. The isosurfaces denote the boundaries of a 99% probability of presence in the last 100 ns-trajectory.

efforts need to be taken to increase the tendency of mixing between the ionic species and COFs and suppress the appearance of ion clusters, which might benefit from mimicking the role of PC molecules in the molecular structure design. The molecular-level engineering of microscopic ion-COF configurations could be key to realizing high-performance, all-solid-state electrolytes.

4. Conclusions

In summary, molecular dynamics simulations with electronic continuum correction were applied to study lithium-ion distribution and motion in the imine-linked TAPB-PDA COF. The efficient force fields enable us to model trajectories as long as 200 ns with experimentally relevant Li loading and propylene carbonate amounts.

$LiClO_4$ tends to form clusters and attach to the walls of the pores of TAPB-PDA COF. Li^+ ions coordinate with the oxygen atoms in ClO_4^- and the nitrogen atoms in the imine linkage, with typical distances of 2.1 Å and 2.2 Å, respectively. The PC molecules blend into the $LiClO_4$ clusters and expand the space that Li^+ can occupy in the TAPB-PDA COF framework. Lithium ions are found to coordinate with the oxygen atoms in PC in a side configuration, with coordination lengths ranging from 2.0 Å to 2.2 Å.

The location of Li^+ is primarily restricted to the $LiClO_4$ clusters, and the formation of continuous transporting pathways is difficult. In comparison to the ionic species, PC molecules are more mobile. Adding PC leads to a more uniform distribution of Li^+ and makes it easier for lithium ions to spread in the pores of the COFs. This helps the formation of continuous ion transport pathways and easier ionic motion inside COFs.

The simulation protocols established here demonstrate efficient modeling of Li-ion motions in COF-based systems, thus being beneficial to the further development of high-throughput molecular screening methods for accelerated

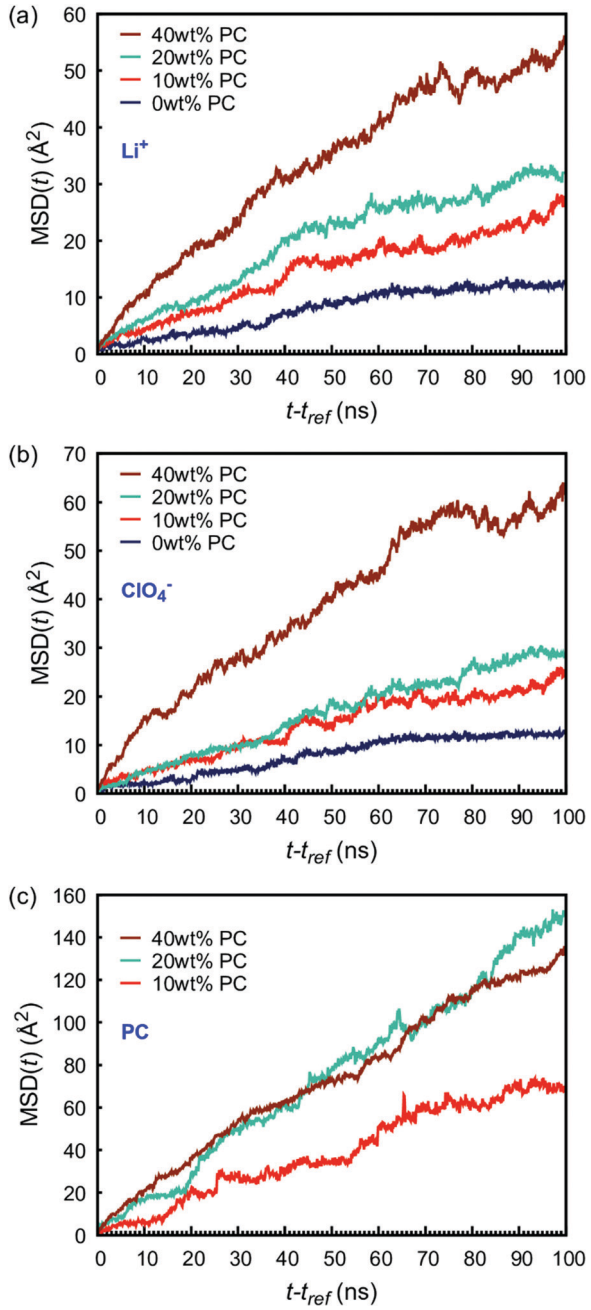

Fig. 7 Mean square deviations in the *z*-direction for (a) Li^+, (b) ClO_4^- and (c) PC at different PC weight ratios.

materials discovery. Overall, these results indicate that, in order to further improve the ionic conductivities of COFs, molecular design and engineering can target suppressing the appearance of ion clusters and promoting the formation of continuous ion transport pathways. Such strategies may benefit from mimicking the role of PC molecules as revealed here.

Conflicts of interest

There are no conflicts to declare.

Acknowledgements

This work was supported by the National Natural Science Foundation of China (grant numbers: 22103053 and 52001124). We would like to thank Prof. Jean-Luc Brédas and Prof. Veaceslav Coropceanu at the University of Arizona for helpful discussions.

References

1 X.-B. Cheng, R. Zhang, C.-Z. Zhao and Q. Zhang, Toward safe lithium metal anode in rechargeable batteries: A review, *Chem. Rev.*, 2017, **117**, 10403.
2 B. Liu, J.-G. Zhang and W. Xu, Advancing lithium metal batteries, *Joule*, 2018, **2**, 833.
3 W. Liu, P. Liu and D. Mitlin, Tutorial review on structure – dendrite growth relations in metal battery anode supports, *Chem. Soc. Rev.*, 2020, **49**, 7284.
4 L. Fan, S. Wei, S. Li, Q. Li and Y. Lu, Recent progress of the solid-state electrolytes for high-energy metal-based batteries, *Adv. Energy Mater.*, 2018, **8**, 1702657.
5 S. Li, S.-Q. Zhang, L. Shen, Q. Liu, J.-B. Ma, W. Lv, Y.-B. He and Q.-H. Yang, Progress and perspective of ceramic/polymer composite solid electrolytes for lithium batteries, *Adv. Sci.*, 2020, **7**, 1903088.
6 R. Chen, Q. Li, X. Yu, L. Chen and H. Li, Approaching practically accessible solid-state batteries: Stability issues related to solid electrolytes and interfaces, *Chem. Rev.*, 2020, **120**, 6820.
7 S.-M. Hao, S. Liang, C. D. Sewell, Z. Li, C. Zhu, J. Xu and Z. Lin, Lithium-conducting branched polymers: New paradigm of solid-state electrolytes for batteries, *Nano Lett.*, 2021, **21**, 7435.
8 X. Li, Q. Hou, W. Huang, H.-S. Xu, X. Wang, W. Yu, R. Li, K. Zhang, L. Wang, Z. Chen, K. Xie and K. P. Loh, Solution-processable covalent organic framework electrolytes for all-solid-state Li–organic batteries, *ACS Energy Lett.*, 2020, **5**, 3498.
9 G. Zhang, Y.-l Hong, Y. Nishiyama, S. Bai, S. Kitagawa and S. Horike, Accumulation of glassy poly(ethylene oxide) anchored in a covalent organic framework as a solid-state Li^+ electrolyte, *J. Am. Chem. Soc.*, 2019, **141**, 1227.
10 K. Jeong, S. Park, G. Y. Jung, S. H. Kim, Y.-H. Lee, S. K. Kwak and S.-Y. Lee, Solvent-free, single lithium-ion conducting covalent organic frameworks, *J. Am. Chem. Soc.*, 2019, **141**, 5880.
11 Y. Hu, N. Dunlap, S. Wan, S. Lu, S. Huang, I. Sellinger, M. Ortiz, Y. Jin, S.-H. Lee and W. Zhang, Crystalline lithium imidazolate covalent organic frameworks with high Li-ion conductivity, *J. Am. Chem. Soc.*, 2019, **141**, 7518.
12 Z. Guo, Y. Zhang, Y. Dong, J. Li, S. Li, P. Shao, X. Feng and B. Wang, Fast ion transport pathway provided by polyethylene glycol confined in covalent organic frameworks, *J. Am. Chem. Soc.*, 2019, **141**, 1923.
13 Q. Xu, S. Tao, Q. Jiang and D. Jiang, Ion conduction in polyelectrolyte covalent organic frameworks, *J. Am. Chem. Soc.*, 2018, **140**, 7429.

14 H. Chen, H. Tu, C. Hu, Y. Liu, D. Dong, Y. Sun, Y. Dai, S. Wang, H. Qian, Z. Lin and L. Chen, Cationic covalent organic framework nanosheets for fast Li-ion conduction, *J. Am. Chem. Soc.*, 2018, **140**, 896.

15 Y. Zhang, J. Duan, D. Ma, P. Li, S. Li, H. Li, J. Zhou, X. Ma, X. Feng and B. Wang, Three-dimensional anionic cyclodextrin-based covalent organic frameworks, *Angew. Chem., Int. Ed.*, 2017, **56**, 16313.

16 D. A. Vazquez-Molina, G. S. Mohammad-Pour, C. Lee, M. W. Logan, X. Duan, J. K. Harper and F. J. Uribe-Romo, Mechanically shaped two-dimensional covalent organic frameworks reveal crystallographic alignment and fast Li-ion conductivity, *J. Am. Chem. Soc.*, 2016, **138**, 9767.

17 A. P. Cote, A. I. Benin, N. W. Ockwig, M. O'Keeffe, A. J. Matzger and O. M. Yaghi, Porous, crystalline, covalent organic frameworks, *Science*, 2005, **310**, 1166.

18 X. Feng, X. S. Ding and D. L. Jiang, Covalent organic frameworks, *Chem. Soc. Rev.*, 2012, **41**, 6010.

19 D. C. Wu, F. Xu, B. Sun, R. W. Fu, H. K. He and K. Matyjaszewski, Design and preparation of porous polymers, *Chem. Rev.*, 2012, **112**, 3959.

20 J. W. Colson and W. R. Dichtel, Rationally synthesized two-dimensional polymers, *Nat. Chem.*, 2013, **5**, 453.

21 S. Y. Ding and W. Wang, Covalent organic frameworks (COFs): From design to applications, *Chem. Soc. Rev.*, 2013, **42**, 548.

22 X. Li and K. P. Loh, Recent progress in covalent organic frameworks as solid-state ion conductors, *ACS Mater. Lett.*, 2019, **1**, 327.

23 K. Xu, Nonaqueous liquid electrolytes for lithium-based rechargeable batteries, *Chem. Rev.*, 2004, **104**, 4303.

24 K. Xu, Electrolytes and interphases in Li-ion batteries and beyond, *Chem. Rev.*, 2014, **114**, 11503.

25 Z. Li, Z.-W. Liu, Z. Li, T.-X. Wang, F. Zhao, X. Ding, W. Feng and B.-H. Han, Defective 2D covalent organic frameworks for postfunctionalization, *Adv. Funct. Mater.*, 2020, **30**, 1909267.

26 Y. Du, H. Yang, J. M. Whiteley, S. Wan, Y. Jin, S.-H. Lee and W. Zhang, Ionic covalent organic frameworks with spiroborate linkage, *Angew. Chem., Int. Ed.*, 2016, **55**, 1737.

27 K. Zhang, B. Zhang, M. Weng, J. Zheng, S. Li and F. Pan, Lithium ion diffusion mechanism in covalent organic framework based solid state electrolyte, *Phys. Chem. Chem. Phys.*, 2019, **21**, 9883.

28 H. Y. Li and J.-L. Brédas, Large out-of-plane deformations of two-dimensional covalent organic framework (COF) sheets, *J. Phys. Chem. Lett.*, 2018, **9**, 4215.

29 C. M. Thompson, G. Occhialini, G. T. McCandless, S. B. Alahakoon, V. Cameron, S. O. Nielsen and R. A. Smaldone, Computational and experimental studies on the effects of monomer planarity on covalent organic framework formation, *J. Am. Chem. Soc.*, 2017, **139**, 10506.

30 M. G. Schwab, M. Hamburger, X. Feng, J. Shu, H. W. Spiess, X. Wang, M. Antonietti and K. Müllen, Photocatalytic hydrogen evolution through fully conjugated poly(azomethine) networks, *Chem. Commun.*, 2010, **46**, 8932.

31 B. J. Smith, A. C. Overholts, N. Hwang and W. R. Dichtel, Insight into the crystallization of amorphous imine-linked polymer networks to 2D covalent organic frameworks, *Chem. Commun.*, 2016, **52**, 3690.

32 C. H. Feriante, S. Jhulki, A. M. Evans, R. R. Dasari, K. Slicker, W. R. Dichtel and S. R. Marder, Rapid synthesis of high surface area imine-linked 2D covalent organic frameworks by avoiding pore collapse during isolation, *Adv. Mater.*, 2020, **32**, 1905776.

33 H. Y. Li and J.-L. Brédas, Nanoscrolls formed from two-dimensional covalent organic frameworks, *Chem. Mater.*, 2019, **31**, 3265.

34 H. Y. Li and J.-L. Brédas, Impact of structural defects on the elastic properties of two-dimensional covalent organic frameworks (2D COFs) under tensile stress, *Chem. Mater.*, 2021, **33**, 4529.

35 I. V. Leontyev and A. A. Stuchebrukhov, Electronic continuum model for molecular dynamics simulations, *J. Chem. Phys.*, 2009, **130**, 085102.

36 I. V. Leontyev and A. A. Stuchebrukhov, Electronic continuum model for molecular dynamics simulations of biological molecules, *J. Chem. Theory Comput.*, 2010, **6**, 1498.

37 L. Martinez, R. Andrade, E. G. Birgin and J. M. Martinez, PACKMOL: A package for building initial configurations for molecular dynamics simulations, *J. Comput. Chem.*, 2009, **30**, 2157.

38 W. L. Jorgensen, D. S. Maxwell and J. TiradoRives, Development and testing of the OPLS all-atom force field on conformational energetics and properties of organic liquids, *J. Am. Chem. Soc.*, 1996, **118**, 11225.

39 H. Y. Li, A. D. Chavez, H. F. Li, H. Li, W. R. Dichtel and J.-L. Brédas, Nucleation and growth of covalent organic frameworks from solution: The example of COF-5, *J. Am. Chem. Soc.*, 2017, **139**, 16310.

40 B. Doherty, X. Zhong, S. Gathiaka, B. Li and O. Acevedo, Revisiting OPLS force field parameters for ionic liquid simulations, *J. Chem. Theory Comput.*, 2017, **13**, 6131.

41 C. M. Breneman and K. B. Wiberg, Determining atom-centered monopoles from molecular electrostatic potentials. The need for high sampling density in formamide conformational analysis, *J. Comput. Chem.*, 1990, **11**, 361.

42 J.-D. Chai and M. Head-Gordon, Long-range corrected hybrid density functionals with damped atom–atom dispersion corrections, *Phys. Chem. Chem. Phys.*, 2008, **10**, 6615.

43 J. Melcr and J.-P. Piquemal, Accurate biomolecular simulations account for electronic polarization, *Front. Mol. Biosci.*, 2019, **6**, 143.

44 K. Nishikawa, Y. Fukunaka, T. Sakka, Y. H. Ogata and J. R. Selman, Measurement of $LiClO_4$ diffusion coefficient in propylene carbonate by Moiré pattern, *J. Electrochem. Soc.*, 2006, **153**, A830.

45 S. Pronk, S. Pall, R. Schulz, P. Larsson, P. Bjelkmar, R. Apostolov, M. R. Shirts, J. C. Smith, P. M. Kasson, D. van der Spoel, B. Hess and E. Lindahl, GROMACS 4.5: A high-throughput and highly parallel open source molecular simulation toolkit, *Bioinformatics*, 2013, **29**, 845.

46 U. Essmann, L. Perera, M. L. Berkowitz, T. Darden, H. Lee, L. G. Pedersen and A. Smooth, Particle Mesh Ewald method, *J. Chem. Phys.*, 1995, **103**, 8577.
47 G. Bussi, D. Donadio and M. Parrinello, Canonical sampling through velocity rescaling, *J. Chem. Phys.*, 2007, **126**, 014101.
48 W. G. Hoover, Canonical dynamics – equilibrium phase-space distributions, *Phys. Rev. A: At., Mol., Opt. Phys.*, 1985, **31**, 1695.
49 D. Ernst and J. Köhler, Measuring a diffusion coefficient by single-particle tracking: Statistical analysis of experimental mean squared displacement curves, *Phys. Chem. Chem. Phys.*, 2013, **15**, 845.
50 M. Park, X. Zhang, M. Chung, G. B. Less and A. M. Sastry, A review of conduction phenomena in Li-ion batteries, *J. Power Sources*, 2010, **195**, 7904.